Nandrolone Decanoate supplementation promotes AMPK activation and divergent brain connectivity rearrangements in adult and aged mice.

Authors: Strogulski, N.S[1]; Kopczinski, A[1]; De Oliveira, V.G.; Carteri, R.B[1]; Sartor, M[1]; Hansel, G[2]; Venturin, G.T[3]; Greggio, S[3]; da Costa, J.C[3]; Rodolphi, M.S[1]; Portela, L.V[1].

[1] Departamento de Bioquímica, ICBS, Universidade Federal do Rio Grande do Sul, Porto Alegre, Brazil.

[2] Penn Center for Brain Injury and Repair and Department of Neurosurgery, Perelman School of Medicine, University of Pennsylvania, Philadelphia,
Pennsylvania 19104

[3] Brain Institute of Rio Grande do Sul (BraIns), Pontifical Catholic University of Rio Grande do Sul (PUCRS), Porto Alegre, RS, Brazil

Abstract

Abnormalities in energetic and proteic homeostasis during ageing relate to neurodegenerative diseases. The mitochondria are a hub of oxidative metabolism, influencing autophagic flux. Ageing can lead to a functional disruption of these systems, leading to neuroenergetic and proteotoxic imbalance. Lower levels of testosterone have been proposed as a mechanism accelerating functional decline during ageing. In this study we investigated whether nandrolone decanoate (ND), an analog of testosterone, in aged animals improves mitochondrial bioenergetics and autophagy. Albino CF1 mice of 3 and 18 months of age, were separated in 4 groups that received daily subcutaneous injections for 15 days of either ND (15mg/kg), or vehicle. Were performed baseline and 14th day ^{18}FDG uptake analysis, through positron emission tomography scan. High resolution respirometry was performed to assess functionally mitochondrial respiratory states and respiratory control ratio (RCR) in synaptossomes fractions. Also, hypothalamic immunocontent of AMPK and pAMPK^{T172}, was assessed. Results demonstrate that Nandrolone increased AMPK activation in both adult and aged mice, but increased ^{18}FDG uptake and mitochondrial basal respiration only in adult mice. Also, Nandrolone triggered a large rearrangement in the metabolic connectivity of adult mice, with a blunted effect over aged mice compared to controls. This suggests that nandrolone promotes diverging adaptations in the metabolism of adult and ageing brain, and that this mechanism is AMPK-independent.

Key-words: Ageing, Mitochondrial Bioenergetics, FDG-PET, Nandrolone

INTRODUCTION

The ageing process has been associated with progressive decrease in physiological functions, including abnormal nutrient sensing and cerebral hypometabolism. An exacerbation of these biochemical features may evolve to compromised synaptic integrity and connectivity, leading to neurofunctional deficits [1].

Particularly, hypothalamus presents a unique role integrating brain and the whole-body energy metabolism. Hypothalamic cells are sensitive to systemic metabolic signals, such as glucose, fatty acids, and hormones like insulin and leptin[2,3]. Intracellularly, a molecular effector of these energy fluctuations and endocrine regulation is the AMP dependent kinase (AMPK). Once activated, AMPK promotes increased glucose uptake, as well as induction of metabolic pathways leading to ATP production [4–6]. This allows AMPK to dynamically respond to changes in synaptic activity and energy demands, mainly through modulation of substrates flow towards mitochondrial oxidative phosphorylation.

As a metabolic hub connecting different cellular functions, mitochondrial dysfunction is believed to contribute for key components leading to cell senescence such as exacerbated oxidative stress, and promotion of apoptosis. Based in this, mitochondrial impairment at nerve terminals, favors the rupture of synaptic function.

The maintenance of healthy synapses relies on adequate mitochondrial function, but also sufficient substrate inflow. Clinically, hallmark neuroimaging findings in aging and age-related disorders, include cerebral hypometabolism detected by fluorodeoxyglucose. Associated to reduced topographical glucose uptake in the brain, diseases common in elder population such as Alzheimer and Parkinson lead to reduced cerebral connectivity assessed by PET-FDG, reflecting neuronal loss and synaptic dysfunction. Interestingly, abnormal energetic homeostasis during aging

parallel with altered hypothalamic activity [7,8], as well as with reduction in the hypophysis-hypothalamic-gonadal signalling, leading to lower testosterone levels in males [9].

This concept has been the mechanistic basis to propose exogenous administration of androgenic anabolic steroids (AAS) [10] to improve bioenergetic mechanisms in peripheral tissues [11–14]. However, although testosterone synthetic analogs replacement therapy has been considered to decrease aging processes, its potential benefits to cerebral connectivity, hypothalamic mechanisms of metabolic control during ageing remains elusive, as well as if these effects are impacted by ageing. Nandrolone Decanoate, is a synthetic analog of testosterone, with robust anabolic effect, that has been previously shown to promote adaptations in synaptic bioenergetics and function [15–17]. Further, the administration of androgen hormones has already been investigated to attenuate cognitive damage following brain injury [18]. Although the abuse of nandrolone for performance and aesthetical purposes has been fairly popularized among young adults, with known behavioural effects, the impacts of its use in cerebral connectivity remain elusive; as well as potential benefits to the metabolism of ageing brain remain unexplored.

In this study we sought to investigate whether nandrolone administration, a testosterone synthetic analog, improves cerebral cell metabolism, and alters cerebral connectivity in adult and aged mice.

METHODS

Animal procedures:

Albino CF1 mice of 3, and 18 months of age were randomly selected to receive either subcutaneous administration of a synthetic analog of testosterone, nandrolone decanoate (18m / ND) (Decadurabolin®, Schering-Plough, Brazil) in the dosage of 15mg/kg, or equivalent volume of administration vehicle (Corn oil, Salada™, Bunge, Brazil) once a day for 15 consecutive days. Animals were maintained with in plexiglass cages, with an average of 4 littermates, and *ad libitum* access to water and standard chow, in controlled temperature (22 ±1°C), and lighting (12h light/12h dark, lights on at 7am) conditions. Following pharmacologic treatment animals were sacrificed and left cerebral hemisphere was homogenized for synaptossomes fractionation, which was used for mitochondrial respirometry, and hypothalamus was dissected and homogenized for immunoblotting assays. All procedures were performed with approval of UFRGS ethics committee for animal experimentation (CEUA UFRGS #33762)

Imunnobloting Analysis

Dissected hypothalamic tissue was homogenized in NP-40 homogenizing buffer and submitted to 12 % acrylamide/bis-acrylamide gel electrophoresis SDS-PAGE, transferred and analyzed in nitrocellulose membranes. Membranes were blocked according to each antibody data sheet. 25µg of each sample was submitted to incubation overnight at 4 ºC with AMPKα2 (Cell Signaling®, USA, 1:1000), and pAMPKα2 (T172) (Cell Signaling®, USA, 1:1000) antibodies. After overnight incubation membranes were washed with 1x TTBS and placed in a 1:25000 secondary HRP conjugated IgG anti-rabbit, or anti-mouse solution (GE Healthcare®, Sweden), accordingly to primary antibody datasheet specification. Western blotting analysis was shown as % of control optic density, analyzed using ImageJ software, normalized with

loading control ß-actin HRP-linked primary antibody (1:10000, Sigma-Aldrich®, Saint Louis, MO, USA), according with instruction of the manufacturer.

Synaptossomes Fractionation

Animal's left hemisphere were rapidly dissected and homogenized in 1000 µL of isolation buffer (320mM sucrose, 10mM Tris, 0,1% BSA, pH 7.4) using a 10 mL glass potter. The brain tissue was gently homogenized with 10 strokes. The homogenate was immediately used for respirometry, and protein quantification for the subsequent normalization of oxygen consumption per mg of tissue.

For synaptosomes isolation, homogenized samples were then centrifuged at 1330 ×g for 3 min. The supernatant was carefully retained and then centrifuged at 21,200 ×g for 10 min. The resulting pellet was resuspended, carefully layered on top of a discontinuous Percoll gradient, and centrifuged for 5 min at 30,700 ×g [11, 12]. This results in a synaptosome-enriched band and extra-synaptic mitochondria enriched band. The synaptosomal and mitochondrial fractions were transferred and resuspended in the isolation buffer and centrifuged for additional 16,900 ^{x}g for 10 min. The resulting pellet was resuspended in 2mL isolation buffer and centrifuged at 6,500 ^{x}g for 10 min. The final pellet of synaptosomes fraction was resuspended in a sucrose and Tris buffer (320mM sucrose, 10mM Tris, pH 7.4) and immediately used for further analysis. [19,20]

microPET-Scan analysis

Non-pharmacologically treated mice were submitted to baseline [^{18}F]FDG uptake evaluation using positron emission tomography scans (microPET), performed

at the Brain Institute (Porto Alegre, Rio Grande do Sul, Brazil). The same animals were resubmitted to [^{18}F]FDG uptake scans after 15 days. Prior to both paired scans, animals were fasted overnight, but had *ad libitum* access to water. Animals were placed on a controlled temperature environment, and an intraperitoneal injection of 200µL of [^{18}F]FDG, with radioactive activity of 240µCi approximately, was made, allowing conscious drug uptake for 40 min. Animals were then anesthetized (Ketamine/Xylasine 90mg/kg and 7.5mg/kg respectively) and microPET-Scans performed[21,22]. Acquisition of FDG-PET images was mapped and quantified as SUV according to *mirrione*[23],and expressed as the variation between paired baseline and 15 days scans. Glucose uptake in the brain was topographically assessed in the following regions: (**RSTR; LSTR**: Striatum, right and left respectively.) (**CTX:** Cortex) (**RHIP; LHIP:** Hippocampus, right and left respectively) (**THA:** Thalamus) (**CB:** Cerebellum) (**BFS:** Basal Forebrain & Septum) (**HYP:** Hypothalamus) (**RAMY; LAMY**: Amygdala, right and left respectively) (**BS:** Brainstem) (**CG:** Cingulate Gyrus) (**SC**: Superior Colliculi) (**OLF:** Olfactoy bulb) (**RMID; LMID:** Midbrain, right and left respectively) (**RIC; LIC:** Inferior Colliculi, right and left respecitively).

High Resolution Respirometry Analysis

High resolution respirometry was performed using an O2k Oxygraph (Oroboros Instuments, Innsbruck, Austria) utilizing a SUIT (substrate, uncoupler inhibitor titration) protocol to assess specific mitochondrial respiratory states as described by Chance *et al* [24], and redefined by Gnaiger *et al* [25]. Synaptossomes obtained from the left cerebral hemisphere were submitted to a high resolution respirometric analysis, using an O2k oxygraph (Oroboros Instuments, Innsbruck, Austria). The analysis was performed in 300 µL of synaptossomes fraction suspended to 2mL of respiration buffer (KCl 100

mM, mannitol 75 mM, sucrose 25 mM, KH_2PO_4 5 mM, EDTA 0.05 mM, and Tris-HCl 10 mM, pH 7.4).

ROUTINE respiration state was reached after the stabilization of oxygen consumption rates following sample addition and is sustained by the endogenous energy substrates. After ROUTINE state was achieved, K CN(1mM) was added to inhibit complex IV, that limits oxygen consumption to non-oxidative reactions, allowing to estimate ROX. Basal respiration was then estimated by the difference between ROX and ROUTINE states.

Statistical Analysis

Due to the nature of the presented data, multiple comparisons One-way or Two-way Analysis of Variance (ANOVA) were performed where applicable, followed by *post hoc* Tuckey test, with significance being considered when $p<0.05$, and normality assessed according to Kolgomorov-Smirnov normality statistical test. All results in figures are presented as mean ± SD. Pearson tests were performed to investigate correlations between variables using the R package *psych* [26], with Bonferroni correction for multiple correlations. Correlation data are expressed as Pearson's r, and only are shown correlations with $r > 0.9$, and $p<0.01$. We estimated metabolic networks through the correlation of the [18F]FDG uptake values among different brain anatomical regions of interest (ROI). The magnitude of the correlation implies in the existence of a functional association. For this approach, the Pearson's r correlation of SUV's obtained in each anatomical region by microPET analysis was used.

Networks were built using the *RedeR* package. Further, we performed clustering with euclidean distance and complete linkage agglomeration method using the *pvclust* package, 10000 bootstraps and seed 123 parameters were set for

assessing the uncertainty in hierarchical clustering. Additionally, heatmaps were obtained from the correlation plots. Finally, the networks were built using the RedeR package.

RESULTS

Nandrolone attenuated AMPK downregulation in aged mice.

Aged control mice (18m/VEH) display a significant decrease of hypothalamic pAMPK (Thr172)/AMPK, compared to 3m/VEH, whilst nandrolone supplementation 18/ND attenuated aged-induced AMPK downregulation in aged mice (18m / ND) (3m / VEH vs. 18m / VEH p=0.0013; 3m / VEH vs. 18m / ND p=0.0607) 3m / VEH vs. 18m / VEH *p=0.0011; 3m / VEH vs. 18m / ND p=0.0607), (One-way ANOVA Multiple Comparisons, *Post-hoc* Tukey; 3m / VEH, n=5; 18m / VEH n=3; 18m / ND n=5) (Figure 1A and B). This regulatory effect of nandrolone was also observed in adult mice, with pAMPK(Thr172)/AMPK ratio significantly increased in 3m/ND mice compared to 3m/VEH.

Nandrolone supplementation alters oxidative metabolism and glucose metabolism only in adult mice.

Cerebral FDG uptake after 15 days of nandrolone administration was significantly increased up to 1.5 fold in adult mice (3m/ND group), compared to age-matched controls injected with oil vehicle (3m/Veh) in all assessed areas (Figure 2A). Further, this increase in glucose uptake promoted by nandrolone treatment was not observed in aged mice (18m/ND), compared to aged mice injected with oil vehicle (18m/Veh) in any of the assessed cerebral regions (Table 1).

Coupled to FDG analysis, animals synaptosomes obtained from whole cerebral hemisphere were submitted to oxygraphic analysis. Synaptosome preparations of the left cerebral hemisphere presented increased oxygen consumption in adult mice treated with ND (3m/ND), compared to controls (3m/Veh), (One-way ANOVA, *Post-hoc* Tukey, 3m / VEH vs 3m / ND *p=0.007) whilst this increase is not observed in aged mice treated with nandrolone (18m/ND) compared to age-matched controls (18m/Veh) (Figure 2B).

A connectivity analysis using the correlation networks of PET-FDG showed that nandrolone administration in adult mice (3m/ND) promotes a rearrangement of correlations that presents fewer regions, with less intercorrelations, and finally, the loss of entire correlation clusters observed in age-matched controls (3m/Veh) (Figure 3A-D). In contrast, nandrolone treatment in aged mice (18m/ND) did not elicit an expressive loss in the number of regions, nor the degree of integration in the correlation network compared to age-matched controls (18m/Veh).

Discussion

Healthy aging in humans is associated with a disruption in cerebral metabolism, connectivity, and a reduction in hormone levels. Hormonal replacement therapies are largely employed in aged populations for therapeutical purposes, regardless of sex or hormone levels, and are frequently used in adults for aesthetical and performance purposes. The metabolic effects of the therapeutical, and non-therapeutical use of these drugs on the brain of adult and aged populations are widely unknown.

Here we showed that the use of nandrolone induces an increase in AMPK, a key metabolic regulator in hypothalamic tissue. This increase in AMPK activation ($pAMPK^{Thr172}$) following the acute use of steroid hormones has been described in other

tissues, such as human cardiomyocytes[27], skeletal muscle[28], and the hypothalamic arcuate nucleus of guinea pigs [29]. We currently expand this concept by demonstrating that this effect is not restricted only to arcuate nucleus, but may be related to whole hypothalamus, and that it is sustained for at least 14 days, in both adult and aged mice. This modulatory effect of steroid hormones could contribute to attenuate some hallmark features of ageing such as abnormal nutrient sensing, leading to malnourishment in aged individuals. In guinea pigs, the activation of arcuate nucleus AMPK by testosterone treatment leaded to not only adaptations in the orexigenic neuronal network, and feeding patterns, but also to systemic metabolism, increasing body temperature up to 16 hours post injection, through AMPK-dependent mechanisms[29].

The cellular effect of AMPK activation is the promotion of major catabolic pathways, generating endogenous substrates that culminate in increased mitochondrial activity. We showed that nandrolone induces an increased mitochondrial oxidation of endogenous substrates only in adult mice synaptosomes. Steroid hormones are known to synaptic mitochondrial activity, by translocation of cytoplasmic androgen receptors to nuclei, but also directly by binding to mitochondrial receptors. Studies have suggested that synaptic mitochondria of nandrolone treated mice present increased basal mitochondrial membrane potential, and hydrogen peroxide production, a proxy indicator of increased endogenous substrate availability and use [15]. This increase in basal mitochondria respiration is not observed in aged mice. A work published by Holloway *et al* [30] suggests that bioenergetic alterations observed in the skeletal muscle of aged male do not translate directly into respirometric alterations, due to the fact that alterations in the aging bioenergetics may involve an insensitivity of mitochondrial ATP synthase to ADP developed through

lifespan. We corroborate to this notion, by showing that albeit ND treatment promotes increased AMPK activation, this does not translate to equivalent elevation in mitochondrial activity.

Hypothalamic AMPK is known to regulate metabolism and glucose uptake of not only peripheral organs, but also other cerebral regions. No previous works have addressed the central effects of steroids in rodent glucose metabolism. In humans, testosterone has been described to increase FDG-uptake, thus restoring regional hypometabolism in the brain of both male and female adult humans [12,31]. These findings also align with the expected outcome of increased AMPK activation decurrent of steroid use. Our study showed that ND supplementation in adult mice induced increases in cerebral FDG uptake, which expands the findings in other species regarding the endogenous androgen hormone to nandrolone as well.

Curiously, our results showed that ND did not benefit aged mice in terms of FDG uptake, which is a result that has not been previously reported in the literature. The effect of testosterone replacement therapy (TRT) on FDG uptake in either cognitively-impaired Alzheimer disease patients or eugonadal patients was already investigated. These studies showed that TRT induced increases in cerebral FDG uptake in these patients [32,33]. Hence, the differences observed between our results regarding the androgen hormones mediating FDG uptake and hypometabolism may shed light onto different brain metabolic responses between aged human and mice.

Albeit the increase of cerebral glucose uptake by nandrolone was restricted to adult mice, the use of nandrolone led to a disruption of cerebral metabolic networks regardless of age. Reductions in connectivity patterns in response to androgen steroid hormones have been shown for a long time in MRI and fMRI studies. Studies have shown that in women injected with testosterone show a reduced functional

connectivity between inferior frontal gyrus and the anterior cingulate cortex, associated with poorer performance in 'Reading the Mind in the Eyes' test [34]. This may suggest that not only steroid hormones promote a loss of connectivity in blood flow, but also in substrate uptake, in response to an increased energy requirement to sustain anabolic processes.

Conclusion

Taken together, the increase in AMPK activation led by nandrolone use, could sustain an increased basal mitochondrial activity by covalent modification of key mitochondrial regulatory enzymes. This increased fuel requirement reflects in increased substrate uptake and oxidation in the whole cerebral tissue. Further, the absence of increased mitochondrial activity, and cerebral glucose uptake, corroborates to suggest a reduction in the sensitivity of aged tissue to AMPK signalling. Interestingly, although the overall metabolic demand has not been altered in aged mice, we showed that changes in metabolic connectivity occur, and that thus could be independent of AMPK regulation.

References:

1. López-Otín, C., Blasco, M. A., Partridge, L., Serrano, M. & Kroemer, G. The Hallmarks of Aging. *Cell* **153**, 1194–1217 (2013).

2. Andersson, U. *et al.* AMP-activated protein kinase plays a role in the control of food intake. *J. Biol. Chem.* **279**, 12005–8 (2004).

3. Dagon, Y. *et al.* p70S6 Kinase Phosphorylates AMPK on Serine 491 to Mediate Leptin's Effect on Food Intake. *Cell Metab.* **16**, 104–112 (2012).

4. Barnes, K. *et al.* Activation of GLUT1 by metabolic and osmotic stress: potential involvement of AMP-activated protein kinase (AMPK). *J. Cell Sci.* **115**, 2433–42 (2002).

5. Merrill, G. F., Kurth, E. J., Hardie, D. G. & Winder, W. W. AICA riboside increases AMP-activated protein kinase, fatty acid oxidation, and glucose uptake in rat muscle. *Am. J. Physiol.* **273**, E1107-12 (1997).

6. Habets, D. D. J. *et al.* Crucial role for LKB1 to AMPKalpha2 axis in the regulation of CD36-mediated long-chain fatty acid uptake into cardiomyocytes. *Biochim. Biophys. Acta* **1791**, 212–9 (2009).

7. Kakimoto, A. *et al.* Age-Related Sex-Specific Changes in Brain Metabolism and Morphology. 221–226 (2016) doi:10.2967/jnumed.115.166439.

8. Brendel, M. *et al.* Time Courses of Cortical Glucose Metabolism and Microglial Activity Across the Life-Span of Wild-Type Mice: A PET Study. *J. Nucl. Med.* **49**, jnumed.117.195107 (2017).

9. Mitchell, R., Hollis, S., Rothwell, C. & Robertson, W. R. Age related changes in the pituitary-testicular axis in normal men; lower serum testosterone results from decreased bioactive LH drive. *Clin Endocrinol* **42**, 501–507 (1995).

10. Brown-Séquard, C. Du role physiologique et thérapéutique d'un suc extrait de testicules d'animaux d'après nombre des faix observés chez l'homme. *Arch. Physiol. Norm. Pathol.* **1**, 739–746 (1899).

11. Bahrke, M. S., Iip, E. Y. & Wright, J. E. Psychological and Behavioural Effects

of Endogenous Testosterone and Anabolic-Androgenic Steroids. **22**, 367–390 (1996).

12. Miller, K. K. *et al.* Testosterone administration attenuates regional brain hypometabolism in women with anorexia nervosa. **132**, 197–207 (2004).
13. Howell, S. J., Radford, J. A., Smets, E. M. A. & Shalet, S. M. Fatigue, sexual function and mood following treatment for haematological malignancy: the impact of mild Leydig cell dysfunction. *British Journal of Cancer* vol. 82 789–793 (2000).
14. Burris, A., Banks, S., Carter, C., Davidson, J. & Sherins, R. A Long-term, Prospective Study of the Physiologic and Behavioural Effects of Hormone Replacement in Untreated Hypogonadal Men. *J. Androl.* **13**, 297–304 (1992).
15. Carteri, R. B. *et al.* Anabolic-androgen steroids effects on bioenergetics responsiveness of synaptic and extrasynaptic mitochondria. *Toxicol. Lett.* **307**, 72–80 (2019).
16. Rodolphi, M. S. *et al.* Glutamate transporter-1 link astrocytes with heightened aggressive behavior induced by steroid abuse in male CF1 mice. *Horm. Behav.* **127**, 104872 (2021).
17. Kalinine, E. *et al.* Nandrolone-induced aggressive behavior is associated with alterations in extracellular glutamate homeostasis in mice. *Horm. Behav.* **66**, 383–392 (2014).
18. Carteri, R. B. *et al.* Testosterone Administration after Traumatic Brain Injury Reduces Mitochondrial Dysfunction and Neurodegeneration. *J. Neurotrauma* **36**, 2246–2259 (2019).
19. Sims, N. R. & Anderson, M. F. Isolation of mitochondria from rat brain using Percoll density gradient centrifugation. *Nat. Protoc.* **3**, 1228–1239 (2008).

20. Sims, N. R. Rapid isolation of metabolically active mitochondria from rat brain and subregions using Percoll density gradient centrifugation. *J. Neurochem.* **55**, 698–707 (1990).

21. Zanirati, G. *et al.* Depression comorbidity in epileptic rats is related to brain glucose hypometabolism and hypersynchronicity in the metabolic network architecture. *Epilepsia* (2018) doi:10.1111/epi.14057.

22. Silva, R. B. M. *et al.* Beneficial Effects of the Calcium Channel Blocker CTK 01512-2 in a Mouse Model of Multiple Sclerosis. *Mol. Neurobiol.* 1–21 (2018) doi:10.1007/s12035-018-1049-1.

23. Mirrione, M. M., Schiffer, W. K., Siddiq, M., Dewey, S. L. & Tsirka, S. E. PET imaging of glucose metabolism in a mouse model of temporal lobe epilepsy. *Synapse* **59**, 119–121 (2006).

24. CHANCE, B. & WILLIAMS, G. R. Respiratory enzymes in oxidative phosphorylation. I. Kinetics of oxygen utilization. *J. Biol. Chem.* **217**, 383–93 (1955).

25. Gnaiger, E. & Gnaiger, E. *Mitochondrial Pathways and Respiratory Control An Introduction to OXPHOS Analysis Mitochondrial Pathways and Respiratory Control An Introduction to OXPHOS Analysis*. (2012).

26. Revelle, W. psych: Procedures for Psychological, Psychometric, and Personality Research. (2018).

27. Troncoso, M. F. *et al.* Testosterone activates glucose metabolism through AMPK and androgen signaling in cardiomyocyte hypertrophy. *Biol. Res.* **54**, 3 (2021).

28. Ghanim, H. *et al.* Testosterone Increases the Expression and Phosphorylation of AMP Kinase α in Men With Hypogonadism and Type 2 Diabetes. *J. Clin.*

Endocrinol. Metab. **105**, 1169–1175 (2020).

29. Borgquist, A., Meza, C. & Wagner, E. J. The role of AMP-activated protein kinase in the androgenic potentiation of cannabinoid-induced changes in energy homeostasis. 482–495 (2015) doi:10.1152/ajpendo.00421.2014.
30. Holloway, G. P. *et al.* Age-Associated Impairments in Mitochondrial ADP Sensitivity Contribute to Redox Stress in Senescent Human Skeletal Muscle. *Cell Rep.* **22**, 2837–2848 (2018).
31. Zitzmann, M., Weckesser, M., Schober, O. & Nieschlag, E. Changes in cerebral glucose metabolism and visuospatial capability in hypogonadal males under testosterone substitution therapy. *Exp. Clin. Endocrinol. Diabetes* **109**, 302–304 (2001).
32. Tan, R. S. Testosterone effect on brain metabolism in elderly patients with Alzheimer's disease: comparing two cases at different disease stages. *Aging Clin. Exp. Res.* **25**, 343–7 (2013).
33. Maki, P. M. *et al.* Intramuscular testosterone treatment in elderly men: evidence of memory decline and altered brain function. *J. Clin. Endocrinol. Metab.* **92**, 4107–14 (2007).
34. Bos, P. A. *et al.* Testosterone reduces functional connectivity during the 'Reading the Mind in the Eyes' Test. *Psychoneuroendocrinology* **68**, 194–201 (2016).

Figures subtitles:

Fig. 1: AMPK activation in the hypothalamus. (A) pAMPK(T172)/AMPK immunocontent ratio is significantly lower in aged animals, relative to controls (3m / VEH) and was attenuated by ND supplementation. (3m / VEH vs. 18m / VEH

*p=0.0011; 3m / VEH vs. 18m / ND p=0.0607), (One-way ANOVA Multiple Comparisons, *Post-hoc* Tukey; 3m / VEH, n=5; 18m / VEH n=3; 18m / ND n=5) **(B)** Representative western blotting membrane of AMPK, pAMPK(T172) and loading control β-actin. Results are presented as mean ± SEM.

Fig. 2: Mitochondrial respiration and FDG uptake. (A) The routine oxygen consumption rate as % of control (3m / VEH), where alterations were only observed on adult animals submitted to ND supplementation (One-Way ANOVA *Post-hoc* Tukey, 3m / VEH vs 3m / ND *p=0.007; 3m / VEH, n=8; 3m / ND, n=3; 18m / VEH n=4; 18m / ND n=5) Results presented as mean ± SEM. **(B)** FDG uptake values of cerebral structures, showing increased uptake in young animals submitted to ND supplementation as compared to all groups. *p<0.005 (3m / VEH vs. 3m / ND p=0.0005; 3m / ND vs. 18m / VEH p=0.0115; 3m / ND vs. 18m / ND p=0.0038), (Two-Way ANOVA Multiple Comparisons, *Post-hoc* Tukey; 3m / VEH, n=10; 3m / ND, n=5; 18m / VEH n=4; 18m / ND n=5) Results presented as mean variation from baseline FDG uptake.

Fig. 3: Nandrolone triggers metabolic connectivity rearrengements in adult mice. (A, B) The correlation network of control adult mice (A) are drastically disrupted by 14 days treatment with nandrolone (B), exhibiting a expressive loss of connections, nodes and clusters, indicating a compromise of synchronous cerebral activity due. **(C, D)** Nandrolone treatment in aged mice alters connectivity, shifting connections and possibly altering the hierarchy of cerebral interactions, but does not lead to reduced clusters and nodes, indicating a remodelling of connectivity, but not overall loss of connections.

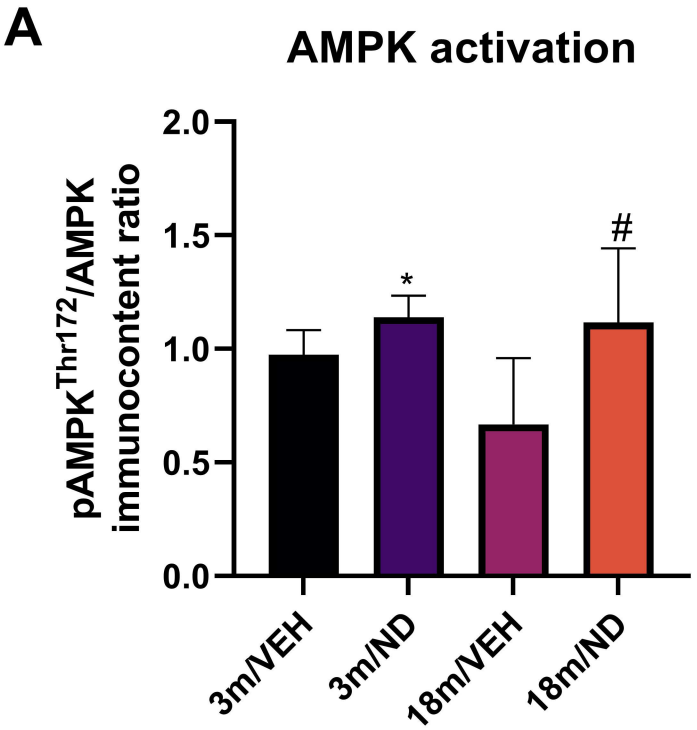
A
AMPK activation
pAMPKThr172/AMPK immunocontent ratio
2.0
1.5
1.0
0.5
0.0
*
#
3m/VEH
3m/ND
18m/VEH
18m/ND

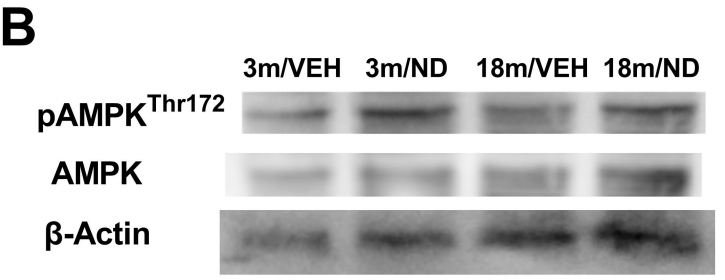
B
3m/VEH
3m/ND
18m/VEH
18m/ND
pAMPKThr172
AMPK
β-Actin

A

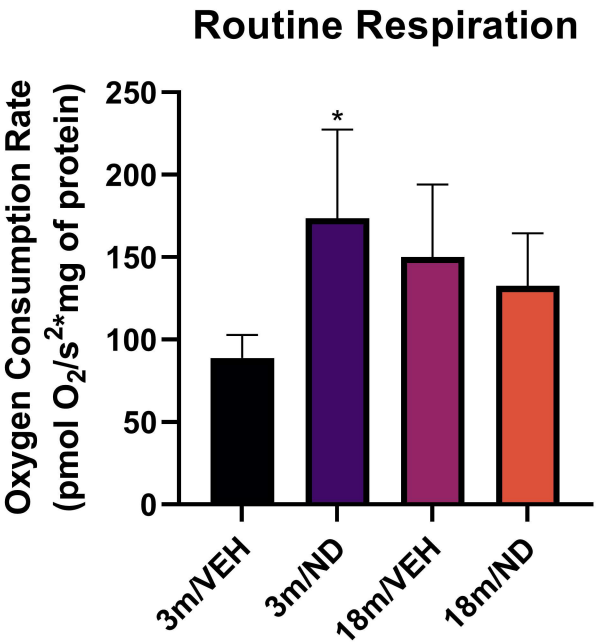
Routine Respiration
Oxygen Consumption Rate
(pmol O2/s2*mg of protein)
250
200
150
100
50
0
*
3m/VEH
3m/ND
18m/VEH
18m/ND

B

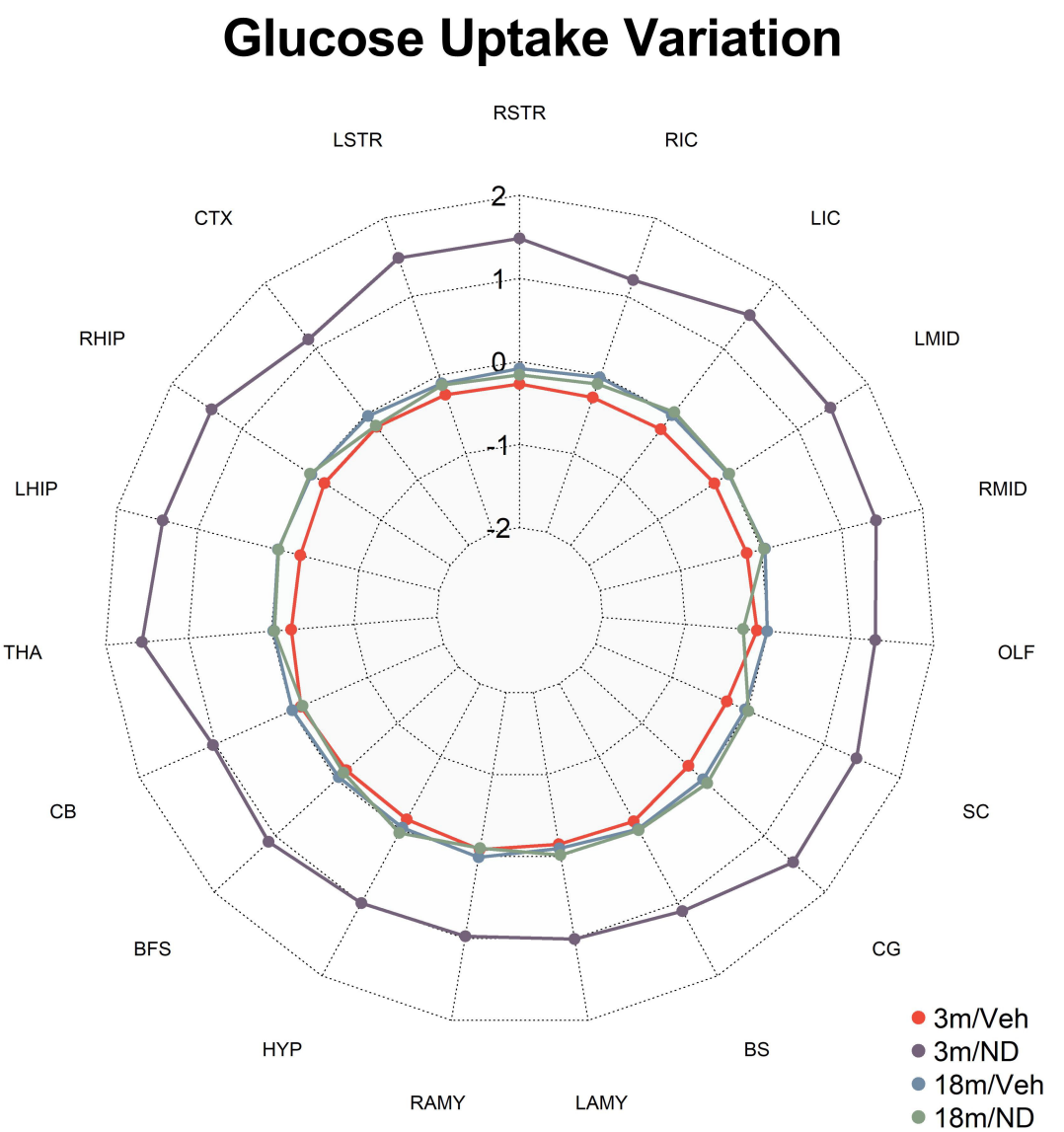
Glucose Uptake Variation
RSTR
RIC
LIC
LMID
RMID
OLF
SC
CG
BS
LAMY
RAMY
HYP
BFS
CB
THA
LHIP
RHIP
CTX
LSTR
2
1
0
-1
-2
3m/Veh
3m/ND
18m/Veh
18m/ND

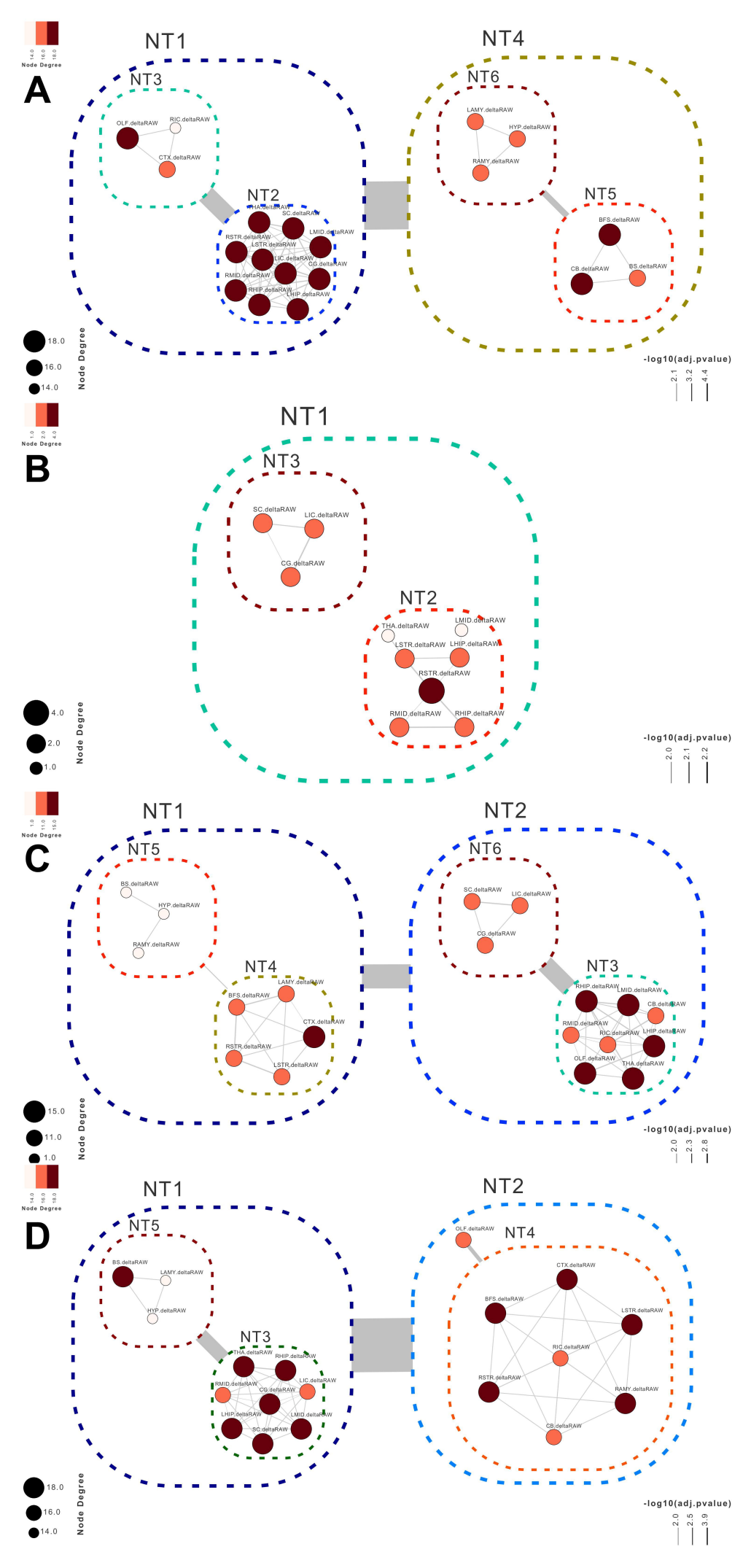
A
NT1
NT3
OLF.deltaRAW
RIC.deltaRAW
CTX.deltaRAW
NT2
THA.deltaRAW
SC.deltaRAW
LMID.deltaRAW
RSTR.deltaRAW
LSTR.deltaRAW
LIC.deltaRAW
CG.deltaRAW
RMID.deltaRAW
RHIP.deltaRAW
LHIP.deltaRAW
NT4
NT6
LAMY.deltaRAW
HYP.deltaRAW
RAMY.deltaRAW
NT5
BFS.deltaRAW
CB.deltaRAW
BS.deltaRAW
Node Degree
18.0
16.0
14.0
-log10(adj.pvalue)
2.1
3.2
4.4
B
NT1
NT3
SC.deltaRAW
LIC.deltaRAW
CG.deltaRAW
NT2
THA.deltaRAW
LMID.deltaRAW
LSTR.deltaRAW
LHIP.deltaRAW
RSTR.deltaRAW
RMID.deltaRAW
RHIP.deltaRAW
Node Degree
4.0
2.0
1.0
-log10(adj.pvalue)
2.0
2.1
2.2
C
NT1
NT5
BS.deltaRAW
HYP.deltaRAW
RAMY.deltaRAW
NT4
LAMY.deltaRAW
BFS.deltaRAW
CTX.deltaRAW
RSTR.deltaRAW
LSTR.deltaRAW
NT2
NT6
SC.deltaRAW
LIC.deltaRAW
CG.deltaRAW
NT3
RHIP.deltaRAW
LMID.deltaRAW
CB.deltaRAW
RMID.deltaRAW
RIC.deltaRAW
LHIP.deltaRAW
OLF.deltaRAW
THA.deltaRAW
Node Degree
15.0
11.0
1.0
-log10(adj.pvalue)
2.0
2.3
2.8
D
NT1
NT5
BS.deltaRAW
LAMY.deltaRAW
HYP.deltaRAW
NT3
THA.deltaRAW
RHIP.deltaRAW
RMID.deltaRAW
LIC.deltaRAW
CG.deltaRAW
LHIP.deltaRAW
LMID.deltaRAW
SC.deltaRAW
NT2
OLF.deltaRAW
NT4
CTX.deltaRAW
BFS.deltaRAW
LSTR.deltaRAW
RIC.deltaRAW
RSTR.deltaRAW
RAMY.deltaRAW
CB.deltaRAW
Node Degree
18.0
16.0
14.0
-log10(adj.pvalue)
2.0
2.5
3.9